Coordination Imperfection Suppressed Phase Stability of Ferromagnetic, Ferroelectric, and Superconductive Nanosolids

Chang Q. Sun,* W. H. Zhong, S. Li, and B. K. Tay

School of Electrical and Electronic Engineering, Nanyang Technological University, Singapore 639798, Singapore

H. L. Bai and E. Y. Jiang

Institute of Advanced Materials and Faculty of Science, Tianjin University, Tianjin 300072, P. R. China

Received: October 31, 2003

Incorporating the recent bond order−length−strength correlation mechanism [Sun; et al. *J. Phys. Chem. B* **2002**, *106*, 10701] into the Ising premise has led to consistent insight, with an analytical expression, into the Curie temperature (T_C) suppression of ferromagnetic, ferroelectric, and superconductive nanosolids. The phase stability is related to the atomic cohesive/exchange energy that is lowered by the coordination number (CN) imperfection of the lower coordinated atoms near the surface edge. A numerical match between predictions and measurements for a number of specimens reveals that the short spin−spin correlation dominates the exchange interaction in the ferromagnetic Fe, Co, Ni, and Fe_3O_2 nanosolids, whereas the long-range interaction dominates the exchange energy for the ferroelectric $PbTiO_3$, $PbZrO_3$, $SrBi_2Ta_2O_9$, and $BaTiO_3$ and the superconductive MgB_2 nanosolids.

1. Introduction

The fascinating physicochemical properties of nanosolids (nanoclusters, nanoparticles, nanocrystallites, or nanomaterials) and the wide possibilities of using these properties in practice have attracted tremendous interest. The Curie temperature (T_C) of ferromagnetic,[1−3] ferroelectric,[4−6] and superconductive[7−9] nanoslids become tunable, which allows us to tune the T_C for switches functioning in a designed temperature range. Numerous models have been developed for the T_C suppression of these materials. For the ferromagnetic nanosolid of radius (for spheres) or thickness (for thin plate) R, or $K = R/d$ atoms of size d lined along the R, the spin−spin correlation length (SSCL, or ξ) limitation mechanism[10] indicates that the T_C suppression is due to the presence of SSCL that is limited by the film thickness or particle size. If the size is smaller than the critical SSCL, the T_C will be lower than the bulk value; otherwise, bulk T_C will remain. The SSCL mechanism gives rise to the step function for the size dependent T_C with λ and ξ as adjustable parameters:[11−15]

$$\frac{\Delta T_C(K)}{T_C(\infty)} = \frac{T_C(K) - T_C(\infty)}{T_C(\infty)} = \begin{cases} -\left(\dfrac{\xi+1}{2K}\right)^{\lambda} & (K > \xi) \\ \dfrac{K-1}{2\xi} - 1 & (K < \xi) \end{cases} \quad (1)$$

Recently, Nikolaev and Shipilin[16] proposed that the ferromagnetic T_C suppression results from nothing more than the surface layer that contains atoms with only half the number of exchange bonds (coordination number (CN) imperfection, as termed in this iteration) per unit volume compared with the bulk. By defining a critical thickness ΔR, the T_C suppression of a ferromagnetic spherical dot can be expressed as follows:[16]

$$\frac{\Delta T_C(R)}{T_C(\infty)} = -\frac{3\Delta R}{2R} \quad (2)$$

The quantity ΔR was used as a parameter to characterize the number deficiency of the exchange bonds for atoms at the surface region of a nanosolid. However, fitting experiment data for Fe_3O_4 nanosolids of different sizes with a constant ΔR was unsuccessful, and hence, it is suggested that the ΔR varies with the solid size, but the R dependence of ΔR needs yet to be established.[16]

For the ferroelectric systems, such as $PbTiO_3$, $BaTiO_3$, $PbZrO_3$, and $BaTiO_3$, three different approaches[17] have been developed to investigate the occurrence of surface modes. They are (1) a microscopic pseudospin theory based on the Ising model in a transverse field, (2) a classical and macroscopic Landau theory in which surface effects can be introduced phenomenologically, and (3) a polariton model appropriate for the very-long-wavelength region. While taking the surface and nonequilibrium energy into consideration, Zhong et al.[18] extended the Landau-type phenomenologically classical theory by introducing a surface extrapolation length δ to the size dependent T_C suppression of ferroelectric nanosolids. However, the model fails to explain the thermal properties of $PbTiO_3$ and $PbZrO_3$ nanosolids. After that, Bursill et al.[19] assumed the phenomenological Landou−Ginzburg−Devonshire coefficients in the Gibbs energy to change with particle size to solve this problem. An empirical equation widely used to fit the T_C suppression of ferroelectric nanosolids is given as[4,5]

$$\Delta T_C(K)/T_C(\infty) = C/(K - K_C) \quad (3)$$

where C and the critical size K_C are adjustable parameters. One may note that if $K = K_C$, eq 3 corresponds to a singularity. Zhong et al.[20] considered the Ising model for the long-range

* Corresponding author. E-mail: ecqsun@ntu.edu.sg. Fax: 65 6792 0415. URL: http://www.ntu.edu.sg/home/ecqsun/.

10.1021/jp0372946 CCC: $27.50
Published on Web 12/18/2003

interaction in dealing with the ferroelectric nanosolids by adjusting the σ in the exchange strength $J_{ij} = J/r_{ij}^{\sigma}$. $\sigma = 0$ corresponds to an infinite-range interaction and $\sigma = \infty$ corresponds to a nearest-neighbor interaction. More recently, Jiang et al.[21] adapted their model for melting point suppression to the T_C suppression of the ferroelectric nanosolids, which is expressed as

$$\frac{\Delta T_C(K)}{T_C(\infty)} = \exp\left(-\frac{2S_0}{R_s}\frac{1}{K/K_C - 1}\right) - 1 \qquad (4)$$

where S_0 is the transition entropy and R_s is the ideal gas constant. Numerical match for the T_C suppression of $BaTiO_3$ and $PbTiO_3$ nanosolids has been reached with the documented S_0 values. It was found by Jiang et al. that the larger K_C value corresponds to a smaller value of S_0.

The Curie temperature of a supeconductive nanosolid is also suppressed by minimizing the particle size. The relation between the T_C and the energy-level spacing for spherical granules was suggested as follows:[22]

$$\ln(T_C(K)/T_C(\infty)) = \sum [2/(2M+1)]\{\tanh[\pi^2(2M+1)k_B T_C/\delta] - 1\} \qquad (5)$$

where k_B is the Boltzmann constant and δ is the energy sublevel splitting in the conduction or valence band that can be estimated with the Kubo formula:[23,24] $\delta = 4E_F/3n \propto 1/V \propto K^{-3}$, where E_F is the fermi energy of the bulk materials and n is the number of valence/conduction electrons in the nanosolid. Index M is the magnetic quantum number. However, the T_C suppression of Pb embedded in the Al−Cu−V matrix measured by Tsai et al.[8] could not fit this prediction. Instead, the trend of Pb T_C suppression follows: $A\exp(-B/K)$, with adjustable constants A and B.

Briefly, the SSCL theory[11] considers the correlation length and the CN imperfection model[16] considers the loss of exchange bonds of atoms in the ferromagnetic surface region. A model for the T_C suppression of superconductive MgB_2 nanosolids[25] is yet lacking. Nevertheless, all the models developed insofar could have contributed significantly to the understanding of T_C suppression from various perspectives. Consistent insight and a unification of the T_C suppression of ferromagnetic, ferroelectric, and superconductive nanosolids is highly desirable. Here we present a model for this purpose by incorporating our recent bond order-length-strength (BOLS) correlation mechanism[26−28] into the Ising model that involves atomic cohesive/exchange energy (atomic coordination number (CN) multiplies the single bond energy).

2. Theory

2.1. Ising Model. For a ferromagnetic nanosolid, the T_C is determined by the spin−spin exchange interaction, $E_{exc,i}$,[14] which is identical to the atomic cohesive energy, $E_{coh,i}$, that sums the bond energy over all the possible coordinates. For a single atom labeled i with z_i coordinates:

$$E_{coh,i} = E_{exc,i} = \sum_{j=1}^{z_i} J_{ij}S_iS_j \propto z_i d_i^{-1} \qquad (6)$$

where S_i and S_j are the total spin or the angular momentum of atoms at the specific site i and its surrounding sites j. The particle size induced momentum change is negligible unless charge transportation or polarization happens in the chemical reaction.[29] J_{ij} is the exchange strength that is proportional to the inverse atomic distance. It is easy to understand that if one needs to disorder the spin−spin interaction by applying a thermal stimulus, one has to provide sufficient energy to lose all the bonds of the atom and to promote the atomic vibration. The total energy, or the exchange interaction, of a specific atom with z_i coordinates, at T, is the sum of all the bond energy and the thermal vibration energy $E_V(T)$.[30] On the other hand, at the Curie temperature, the thermal vibration energy required for disordering the exchange interaction is a portion of the atomic cohesive energy (at $T = 0$).[14] This premise holds for any phase transition including melting and evaporating of an atom in a solid.[30] Therefore,

$$\begin{cases} E_{total}(d,T) & = E_{coh}(d) + E_V(T) = E_{exc}(d,T) \\ T_C & \propto E_{exc}(d,0) \end{cases} \qquad (7)$$

Based on the mean field approximation and Eienstein's relation,[12,31] $E_V(T) = k_B T$. For a ferroelectric system, the exchange energy also follows the Ising model, but the S here stands for the quanta of dipole or ion (may be called quasi-dipole) that are responsible for the ferroelectric performance. In general, we may name such a quanta as a dipole. The difference in the correlation length is that the dipole system is longer than that of a ferromagnetic system. Usually, dipole−dipole Van der Vaals interaction follows the r^{-6} type whereas the superparamagnetic interaction follows r^{-3} form. Hence, it is insufficient to count only the exchange bonds within the nearest neighbors for atoms in a ferroelectric system. A critical exchange correlation radius K_C can be defined to count the contribution from all atoms within the sphere of K_C atoms lined along the radius to the atom in the central point. The sum in eq 6 changes from z_i to a value over all the K_C shells.

2.2. BOLS Correlation. The BOLS correlation indicates that the CN reduction of an atom at a flat or at the curved surface of a nanosolid causes the remaining bonds of the lower-coordinated atoms to contract spontaneously with an association of magnitude increase in bond energy. Hence, the atomic cohesive energy, $E_{coh,i}$ of the lower-coordinated atom will change, which determines the thermodynamic properties such as self-assembly growth, diffusion, chemical reactivity,[32] melting,[30] and phase transition.[14,33] The energy density rise per volume in the relaxed region will contribute to the Hamiltonian that modifies the entire band structure[27,28] and the mechanical strength[32] of a nanosolid. The BOLS correlation and its effect on the cohesive energy per bond and per atom are given as[30]

$$\begin{cases} \{c_i = d_i/d = 2\}/\{1 + \exp[(12 - z_i)/(8z_i)]\} \\ E_i/E_b = c_i^{-m} \\ E_{coh,i}/E_{coh,b} = z_{ib}c_i^{-m} \end{cases} \qquad (8)$$

where d and d_i are the diameters of an atom with z neighbors in the extended solid and an atom with z_i coordinates at the ith atomic layer. The index i is counted from the outermost to the center of the solid. $z_{ib} = z_i/z_b$ is the reduced CN. E_i and E_b are the cohesive energy per bond of an atom with and without CN imperfection. $E_{coh,i} = z_iE_i$ and $E_{coh,b} = z_bE_b$ are the corresponding atomic cohesive energies. The index m changes with the nature of the bond. For a flat or slightly curved surface, $z_1 = 4$, $z_2 = 6$, $z_3 = 8$, and $z_b = 12$ as a standard; for a spherical nanosolid, $z_1 = 4(1 - 0.75/K)$.

2.3. Shell Structure and the Critical Volume V_C. Considering the BOLS correlation in the surface region of a nanosphere with radius R that contains N atoms, the total cohesive energy

of the entire nanosolid can be expressed in a shell structure:

$$E_{coh}(K) = Nz_bE_b + \sum_{i\leq 3} N_i(z_iE_i - z_bE_b) \quad (9)$$

where N_i is number of atoms in the ith surface layer. The term Nz_bE_b is the cohesive energy of the system without involving the effect of CN imperfection. The relative change of the cohesive energy of a nanosolid, or the mean value change of a single atom, follows:

$$\frac{\Delta E_{coh}(K)}{E_{coh}(\infty)} = \sum_{i\leq 3} \frac{N_i}{N}\left(\frac{z_iE_i - zE_b}{zE_b}\right) = \sum_{i\leq 3}\gamma_i(z_{ib}c_i^{-1} - 1) \quad (10)$$

Equation 10 indicates that the relative change of the cohesive energy of a nanosolid originates from the difference in the E_{coh} between a surface atom and a bulk atom: $z_{ib}c_i^{-1} - 1$, due to the BOLS correlation. The trend of change depends on the portion of surface atoms, γ_i, in the first three atomic layers with appreciable CN imperfection.

For a ferroelectric spherical dot with radius $R = Kd$, we need to consider the interaction between the specific central atom and its surrounding neighbors within the critical volume $V_C = 4\pi K_C^3/3$, in addition to the BOLS correlation in the surface region. The ferroelectric property drops down from the bulk value to a value smaller than 5/16 (estimated from Figure 1) when one goes from the central atom to the edge along the radius. If the surrounding volume of the central atom is smaller than the critical V_C, the ferroelectric feature of this central atom attenuates; otherwise, the bulk value remains. For an atom in the ith surface layer, the number of the lost exchange bonds is proportional to the volume V_{vac}, that is, the volume difference between the two caps of the V_C sized spheres, as illustrated in Figure 1a. Therefore, the relative change of the ferroelectric exchange energy of an atom in the ith atomic layer compared to that of a bulk atom becomes

$$\frac{\Delta E_{exc,i}}{E_{exc}(\infty)} = \frac{V_C - V_{vac}}{V_C} - 1 = -\frac{V_{vac}}{V_C} \quad (11)$$

2.4. Generalization of the T_C Suppression. Substituting eq 11 for the $z_{ib}c_i^{-m}$ in eq 10 and considering the BOLS correlation in the surface region, we have a universal form for the T_C suppression for ferromagnetic, ferroelectric, and supercondiuctive nanosolids ($m = 1$ in the Ising model):

$$\frac{\Delta T_{C(R)}}{T_C(\infty)} = \frac{\Delta E_{exc}(R)}{E_{exc}(\infty)} = \begin{cases} \sum_{i\leq 3}\gamma_i(z_{ib}c_i^{-1} - 1) = \Delta_{coh} & \text{ferromagnetic} \\ \sum_{i\leq K_C}\gamma_i\left(\frac{-V_{vac}}{V_C}\right) + \Delta_{coh} = \Delta_{coh} & \text{else} \end{cases} \quad (12)$$

For the short spin−spin interaction, it is sufficient to sum over the outermost three atomic layers whereas for a ferroelectric and a superconductive solid the sum should be within the sphere of radius K_C. Compared with the model given in eq 2, $\Delta R = R\Delta_{coh}$ is not a constant, in particular, at the lower end of the size limit, because γ_i drops from unity to infinitely small when the particle grows from atomic scale to macrometer size.[28−30]

3. Results and Discussion

Least-squares linearization of the measured size dependent T_C represented by eq 3 gives the slope B' and an intercept that corresponds to the bulk $T_C(\infty)$. The measured data may need calibration by matching the intercept to the $T_C(\infty)$. Compared with eq 12, one would find that $B' = R\Delta_{COH}$ for a ferroelectric system and then the adjustable K_C is obtained by computing optimization. For a ferromagnetic system, $B' = R\Delta_{coh}$, without needing numerical optimization. Calculations based on eq 12 were conducted using the following parameters: $z_{1b} = 1/3$, $z_{2b} = 1/2$, and the average bond length and the $T_C(\infty)$ values as listed in Table 1. Figure 2a shows the match of the BOLS predicted lines with the measured size dependent T_C for ferromagnetic Fe,[3] Co,[1] and Ni[13] nanofilms and Fe_3O_4[34] nanospheres. The critical size at which $T_C = 0$ for the ferromagnetic solids is determined is $z_1 = 0$ in eq 12 as $\gamma_1 = 1$, $\gamma_2 = \gamma_3 = 0$, which is the case of an isolated atom.

For ferroelectricic systems, we need to optimize the K_C value in computation to match theoretical curve to the measured data. Figure 2b shows the T_C suppression of ferroelectric $PbTiO_3$,[5] $SrBi_2Ta_2O_9$,[6] $BaTiO_3$,[35] and antiferroelctric $PbZrO_3$[36] nanosolids. Calculations of optimized K_C values for $PbTiO_3$, $PbZrO_3$, $BaTiO_3$, and $SrBi_2Ta_2O_9$ are listed in Table 1. For ferroelectric

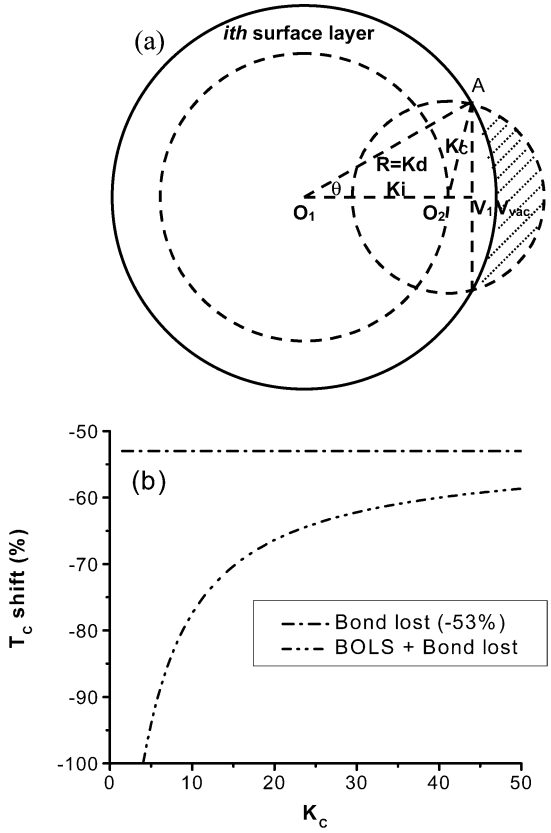

Figure 1. Schematic illustration of the high-order exchange bonds loss of an atom in a spherical nanosolid with radius K ($K = R/d$ is the number of atoms of size d lined along the radius R of a sphere or across a thin plate of R thickness. K_C is the critical correlation radius. The lost V_{vac} (the shaded portion) is calculated by differencing the volumes of the two spherical caps:

$$V_{vac} = \pi(K_C + K_i - K\cos\theta)^2\left(K_C - \frac{K_C + K_i - K\cos\theta}{3}\right) - \pi(K - K\cos\theta)^2\left(K - \frac{K - K\cos\theta}{3}\right)$$

where the angle θ is determined by the triangle O_1O_2A. Critical correlation radius K_C dependence of the T_C shift of ferroelectric and superconductive alloying nanosolids. For the $K_C = 5$ example, bond contraction (BOLS) lowers the T_C by −41.1% (follows the curve in Figure 1a) and the high-order bond lost (Bond lost) contribution that is a constant lowers the T_C by −53% and the overall T_C shift is −94%. $K_C \leq 4$, $T_C = 0$.

TABLE 1: Bulk Atomic Diameter, D, $T_C(\infty)$, and the Critical Correlation Radius (K_C) at Which the Central Atom That Lost Its Ferroelectricity Attenuates[a]

materials	d/nm	$T_C(\infty)$/K	K_C/R_C(nm)	R'_C/nm
Fe	0.252	1043	1	3^0
Co	0.250	1395	1	0^1
Ni	0.248	631	1	0^{13}
Fe_3O_4	0.222	860	1	0^{34}
$PbTiO_3$	0.283	773	4/1.04	6.3,[4] 4.5[5]
$SrBi_2Ta_2O_9$	0.270	605	4/1.0	1.3^6
$PbZrO_3$	0.288	513	8/2.3	15^{36}
$BaTiO_3$	0.243	403	100/24.3	24.5,[38] 55[35]
MgB_2	0.352	41.7	3.5/1.25	1.25^{37}
Pb	0.349	7.2	3.5/1.25	1.25^8

[a] $K_C \leq 4$ corresponds to $T_C = 0$. The critical radius R'_C at which $T_C = 0$ is derived by other models.

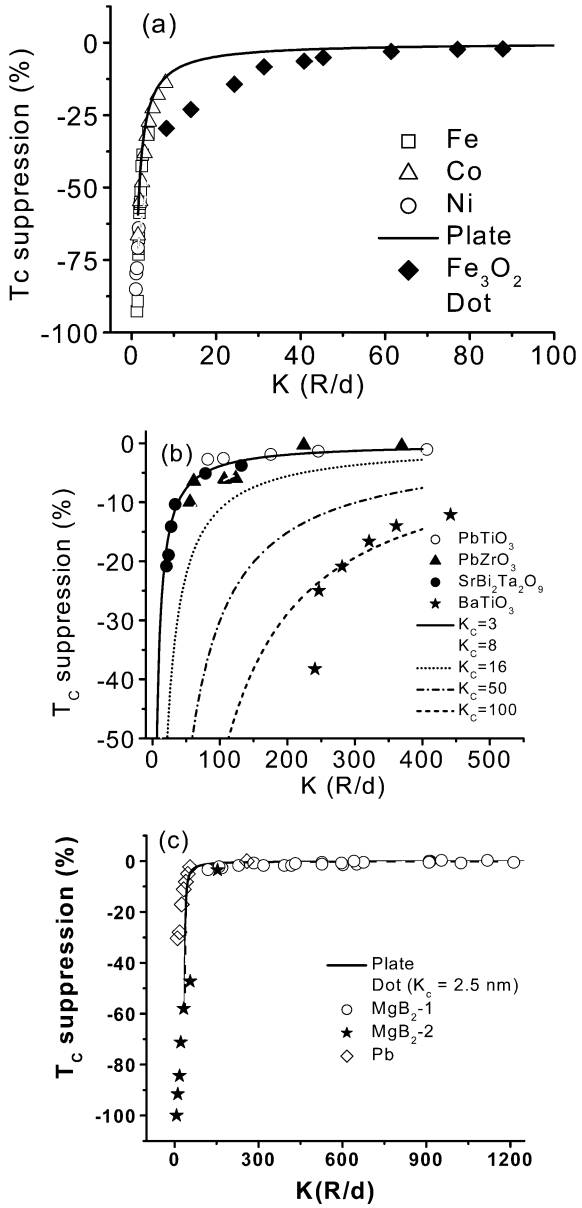

Figure 2. Numerically matching of the predicted with the measured T_C suppression of (a) ferromagnetc Fe,[3] Co,[1] and Ni,[13] nanofilms, and Fe_3O_3 nanodots.[34] Fitting experimental data for ferroelectric (b) $PbTiO_3$,[5] $SrBi_2Ta_2O_9$,[6] $BaTiO_3$,[35] and $PbZrO_3$[36] nanosolids and (c) the superconductive MgB_2-1,[7] MgB_2-2,[37] and Al−Cu−V embedded Pb[8] nanosolids gives the K_C values, as compared with the critical size determined by the empirical approach in Table 1.

and supercondictive nanosolids, $T_C = 0$ happens at $V_{vac} = V_C$, which means that the $K = K_C$ corresponds not to $T_C = 0$ but to a value that is too low to be detected. Figure 1b shows the K_C dependence of the T_C shift. For th $K_C = 5$ example, bond contraction lowers the T_C by −41.1%, the volume loss contribution lowers the T_C by −53%, and the overall T_C shift is −94%. The difference in the optimized K_C by different approaches, as compared in Table 1, lies in that the slope (surface/volume ratio) in the current approach is not a constant but changes with particle size.

Applying the BOLS prediction to the measurement of T_C suppression of superconductive MgB_2 nanosolids (Figure 2c) leads to an estimation of the critical radius $K_C = 3.5$, which agrees with that determined recently by Li et al. ($R_C \sim 1.25$ nm).[37] Consistency of the BOLS prediction with the experiment data indicates that the long-range interaction dominates the superconductive T_C. For Al−Cu−V embedded Pb nanosolid,[8] the K_C is around 1, being the same as that for a ferromagnetic solid. This finding may provide a mechnism for the origin of the superconductive T_C suppression of MgB_2 nanosolids.

4. Conclusion

We have developed a model attempting to unify the T_C suppression of ferromagnetic, ferroelectric, and superconductive nanosolids. Compared with the previous sophisticated modeling exercises, we considered the effect of atomic CN imperfection and its consequence on the atomic cohesive/exchange energy that determines the thermal stability of the nanosolids. We found that considering the BOLS correlation is sufficient for the short spin−spin exchange interaction in ferromagnetic systems whereas for ferroelectric and superconductive alloying nanosolids, the long-range exchange interaction cannot be neglected. Matching between predictions/calculations to experimental observations for these three kinds of nanosolids evidences the validity of the BOLS premise, which provides consistent physical insight into the origin for the T_C suppression for these specimens.

References and Notes

(1) Huang, F.; Kief, M. T.; Mankey, G. J.; Willis, R. F. *Phys. Rev. B* **1994**, *49*, 3962.
(2) Kenning, G. G.; Slughter, J. M.; Cowen, J. A. *Phys. Rev. Lett.* **1997**, *59*, 2596.
(3) Qiu, Z. Q.; Person, J.; Bader, S. D. *Phys. Rev. Lett.* **1993**, *70*, 1006.
(4) Ishikawa, K.; Yoshikawa, K.; Okada, N. *Phys. Rev. B* **1988**, *37*, 5852.
(5) Zhong, W. L.; Jiang, B.; Zhang, P. L.; Ma, J. M.; Cheng, H. M.; Yang, Z. H.; Li, L. X. *J. Phys.: Condens. Matter* **1993**, *5*, 2619.
(6) Yu, T.; Shen, Z. X.; Toh, W. S.; Xue, J. M.; Wang, J. *J. Appl. Phys.* **2003**, *94*, 618.
(7) Pogrebnyakov, A. V.; Redwing, J. M.; Jones, J. E.; Xi, X. X.; Xu, S. Y.; Li, Q.; Vaithyanathan, V.; Schlom, D. G. *Appl. Phys. Lett.* **2003**, *82*, 4319.
(8) Tsai, A. P.; Chandrasekhar, N.; Chattopadhyay, K. *Appl. Phys. Lett.* **1999**, *75*, 1527.
(9) Giaever, I.; Zeller, H. R. *Phys. Rev. Lett.* **1968**, *20*, 1504.
(10) Fisher, M. E.; Barber, M. N. *Phys. Rev. Lett.* **1972**, *28*, 1516.
(11) Richie, D. S.; Fisher, M. E. *Phys. Rev. B* **1973**, *7*, 480.
(12) Zhang, R.; Willis, R. F. *Phys. Rev. Lett.* **2001**, *86*, 2665.
(13) Huang, F.; Mankey, G. J.; Kief, M. T.; Willis, R. F. *J. Appl. Phys.* **1993**, *73*, 6760.
(14) Zhang, R.; Willis, R. F. *Phys. Rev. Lett.* **2001**, *86*, 2665.
(15) Zhong, W. H.; Sun, C. Q.; Tay, B. K.; Li, S.; Bai, H. L.; Jiang, E. Y. *J. Phys.: Condens. Matter* **2002**, *14*, L399.
(16) Nikolaev, V. I.; Shipilin, A. M. *Phys. Solid State* **2003**, *45*, 1079.
(17) Cottam, M. G.; Tilley, D. R.; Zeks, B. *J. Phys. C* **1984**, *17*, 1973.
(18) Zhong, W. L.; Wang, Y. G.; Zhang, P. L.; Qu, B. D. *Phys. Rev. B* **1994**, *50*, 698.
(19) Jiang, B.; Bursill, L. A. *Phys. Rev. B* **1999**, *60*, 9978.
(20) Wang, C. L.; Xin, Y.; Wang, X. S.; Zhong, W. L. *Phys. Rev. B* **2000**, *62*, 11432.
(21) Jiang, Q.; Cui, X. F.; Zhao, M. *Appl. Phys. A* **2002**, *76*, 1.

(22) Muhlschlegel, B.; Scalapino, D. J.; Denton, R. *Phys. Rev. B* **1972**, *6*, 767.

(23) Kubo, R. J. *Phys. Soc. Jpn.* **1962**, *17*, 975.

(24) Sun, C. Q. *Phys. Rev. B*, in press. Surface and Nanosolid Core-level Shift: Impact of Atomic Coordination Number Imperfection.

(25) Strongin. M.; Thompson, R. S.; Karnmerer, O. F.; Crow, J. E. *Phys. Rev. B.* **1970**, *1*, 1078. Coswami, R.; Banerjee, S.; Chattopadhyay, K.; Raychaudhuri, A. K. *J. Appl. Phys.* **1993**, *73*, 2934. Braun, F.; Von, Delft. J. *Phys. Rev. B* **1999**, *59*, 9527.

(26) Sun, C. Q.; Li, S.; Tay, B. K. *Appl. Phys. Lett.* **2003**, *82*, 3568.

(27) Sun, C. Q.; Li, S.; Tay, B. K.; Chen, T. P. *Acta Mater.* **2002**, *50*, 4687.

(28) Sun, C. Q.; Pan, P. K.; Bai, H. L.; Li, Z. Q.; Wu, P.; Jiang, E. Y. *Acta Mater.* **2003**, *51*, 4631.

(29) Sun, C. Q. *Oxidation Electronics. Prog. Mater. Sci.* **2003**, *48*, 521.

(30) Sun, C. Q.; Wang, Y.; Tay, B. K.; Li, S.; Huang, H.; Zhang, Y. *J. Phys. Chem. B* **2002**, *106*, 10701.

(31) Stanley, H. E. *Introduction to Phase Transition and Critical Phenomena*; Oxford University Press: New York, 1971.

(32) Sun, C. Q.; Bai, H. L.; Tay, B. K.; Li, S.; Jiang, E. Y. *J. Phys. Chem. B* **2003**, *107*, 7544.

(33) Huang, H. T.; Sun, C. Q.; Zhang, T. S.; Peter, H. *Phys. Rev. B* **2001**, *63*, 184112.

(34) Sadeh, B.; Doi, M.; Shimizu, T.; Matsui, M. J. *J. Magn. Soc. Jpn.* **2000**, *24*, 511.

(35) Uchina, K.; Sadanaga, Y.; Hirose, T. *J. Am. Ceram. Soc.* **1999**, *72*, 1555.

(36) Soma, C.; Pushan, A.; Palkar, V. R.; Gurjar, A. V.; Wankar, R. M.; Manu, M. *J. Phys.: Condens. Matter* **1997**, *9*, 8135.

(37) Li, S.; While, T.; Sun, C. Q. Unpublished.

(38) Schlag, S.; Eicke, H. F.; Stern, W. B. *Ferroelectrics* **1995**, *173*, 351.